ResearchGate

See discussions, stats, and author profiles for this publication at: https://www.researchgate.net/publication/26832391

On the Nature of the Adsorbed Hydrogen Phase in Microporous Metal-Organic Frameworks at Supercritical Temperatures

ARTICLE *in* LANGMUIR · SEPTEMBER 2009

Impact Factor: 4.46 · DOI: 10.1021/la901680p · Source: PubMed

CITATIONS
14

READS
51

2 AUTHORS:

Eric Poirier
Ford Motor Company
25 PUBLICATIONS **573** CITATIONS
SEE PROFILE

Anne Dailly
General Motors Company
54 PUBLICATIONS **3,767** CITATIONS
SEE PROFILE

Available from: Eric Poirier
Retrieved on: 20 January 2016

NRC-CNRC
From Discovery to Innovation...
De la découverte à l'innovation...
La Science à l'œuvre pour le at work for Canada

NRC Publications Archive (NPArC)
Archives des publications du CNRC (NPArC)

On the Nature of the Adsorbed Hydrogen Phase in Microporous Metal – Organic Frameworks at Supercritical Temperatures

Poirier, Eric; Dailly, Anne

Publisher's version / la version de l'éditeur:
Langmuir, 25, 20, pp. 12169-12176, 2009-09-01

Web page / page Web
http://dx.doi.org/10.1021/la901680p
http://nparc.cisti-icist.nrc-cnrc.gc.ca/npsi/ctrl?action=rtdoc&an=14829323&lang=en
http://nparc.cisti-icist.nrc-cnrc.gc.ca/npsi/ctrl?action=rtdoc&an=14829323&lang=fr

Access and use of this website and the material on it are subject to the Terms and Conditions set forth at
http://nparc.cisti-icist.nrc-cnrc.gc.ca/npsi/jsp/nparc_cp.jsp?lang=en
READ THESE TERMS AND CONDITIONS CAREFULLY BEFORE USING THIS WEBSITE.

L'accès à ce site Web et l'utilisation de son contenu sont assujettis aux conditions présentées dans le site
http://nparc.cisti-icist.nrc-cnrc.gc.ca/npsi/jsp/nparc_cp.jsp?lang=fr
LISEZ CES CONDITIONS ATTENTIVEMENT AVANT D'UTILISER CE SITE WEB.

Contact us / Contactez nous: nparc.cisti@nrc-cnrc.gc.ca.

National Research Council Canada | Conseil national de recherches Canada
Canada

Langmuir
Article
pubs.acs.org/Langmuir
© 2009 American Chemical Society

On the Nature of the Adsorbed Hydrogen Phase in Microporous Metal−Organic Frameworks at Supercritical Temperatures

Eric Poirier*,†,‡,§ and Anne Dailly†

†Chemical and Environmental Sciences Laboratory, General Motors Corporation, Warren, Michigan 48090, and ‡College of Engineering, Purdue University, West Lafayette, Indiana 47907. §Current address: National Research Council Canada, Canadian Neutron Beam Centre, Chalk River Laboratories, Building 459, Station 143C, Chalk River ON, K0J 1J0 Canada.

Received May 12, 2009. Revised Manuscript Received August 24, 2009

Hydrogen adsorption measurements on different metal−organic frameworks (MOFs) over the 0−60 bar range at 50 and 77 K are presented. The results are discussed with respect to the materials' surface area and thermodynamic properties of the adsorbed phase. A nearly linear correlation between the maximum hydrogen excess amount adsorbed and the Brunauer−Emmett−Teller (BET) surface area was evidenced at both temperatures. Such a trend suggests that the adsorbed phase on the different materials is similar in nature. This interpretation is supported by measurements of the adsorbed hydrogen phase properties near saturation at 50 K. In particular it was found that the adsorbed hydrogen consistently exhibits liquid state properties despite significant structural and chemical differences between the tested adsorbents. This behavior is viewed as a consequence of molecular confinement in nanoscale pores. The variability in the trend relating the surface area and the amount of hydrogen adsorbed could be explained by differences in the adsorbed phase densities. Importantly, the latter were found to lie in the known range of bulk liquid hydrogen densities. The chemical composition and structure (e.g., pore size) were found to influence mainly how adsorption isotherms increase as a function of pressure. Finally, the absolute isotherms were calculated on the basis of measured adsorbed phase volumes, allowing for an estimation of the total amounts of hydrogen that can be stored in the microporous volumes at 50 K. These amounts were found to reach values up to 25% higher than their excess counterparts, and to correlate with the BET surface areas. The measurements and analysis in this study provide new insights on supercritical adsorption, as well as on possible limitations and optimization paths for MOFs as hydrogen storage materials.

1. Introduction

The environmental and economical concerns associated with the current use of fossil fuels strongly stimulate research and development on alternate fuels such as hydrogen. In the perspective of a hydrogen-fueled economy, one of the critical issues is the development of a safe, compact, and efficient on-board fuel storage system. Many hydrogen storage strategies are currently under investigation in order to improve on the traditional compression and liquefaction approaches, which have significant efficiency penalties.[1] The adsorption of molecular hydrogen in microporous materials attracts significant interest because it can allow the storage of a larger amount of gas than single compression under given pressure and temperature (P, T). Conversely, it can provide for a lower operating pressure facilitating the use of conformable tanks.[1] In addition, because of weak physical solid−gas interactions, the adsorption mechanism is generally fast and reversible, facilitating the handling of the fuel. The latter characteristics are also critical for on-board application. The hydrogen storage capacity of an adsorbent is determined by its microporous volume and the extent of its surface area. Among the most interesting materials in that respect are the metal−organic frameworks (MOFs). The latter have specific surface areas and micropore volumes that can exceed that of traditional adsorbents such as zeolites and activated carbons. MOFs are hybrid inorganic−organic frameworks that are assembled by the connection of secondary building blocks (SBU), usually consisting of metal ions or clusters, through rigid organic ligands. The variety of cations and molecular bridges that can be combined in the framework yields an extended range of materials with diverse pore sizes and functionalities. Efforts are now being made to tune these adsorbents with properties suited for hydrogen storage applications. In that regard, the extent to which pore geometry and functionality affect the nature of the adsorbed hydrogen phase is a crucial question in determining how these materials can be improved.

Because of their crystalline nature, MOFs offer a well-defined structural platform from which, in principle, the sorption properties and mechanism can be studied. This is illustrated in the Figure 1 and 2 which show how the surface area of IRMOF-1 (Zn(BDC)) is generated by the framework. In this case, the *Connolly* surface was plotted using the Material Studio software. Clearly both the extent of surface area and accessible porous volume appear as determinant factors for the hydrogen storage capacity of a MOF. An important step for the tuning of adsorbents for a specific application is to understand the relationship between the adsorption enthalpy, the surface area and the porous volume. At low pressures the hydrogen uptake correlates with the adsorption enthalpy.[2] This quantity is a measure of the strength of the solid−gas interactions and is determined by the nature of the chemical constituents and the structure of the adsorbent. At higher pressures, i.e., when the excess maximum is reached, hydrogen uptakes can be related to the specific surface area and the porous volume. The Brunauer−Emmett−Teller (BET) specific surface area, along with the micropore volume

*Corresponding author. E-mail: Eric.M.Poirier@nrc.gc.ca. Tel: 613-584-8811 ext. 44179. Fax: 613-584-4040.

(1) Poirier, E.; Chahine, R.; Bénard, P.; Cossement, D.; Lafi, L.; Mélançon, E.; Bose, T. K.; Désilets, S. *Appl. Phys. A: Mater. Sci. Process* **2004**, *78*, 961–967.

(2) Frost, H.; Düren, T.; Snurr, R. S. *J. Phys. Chem. B* **2006**, *110*, 9565–9570.

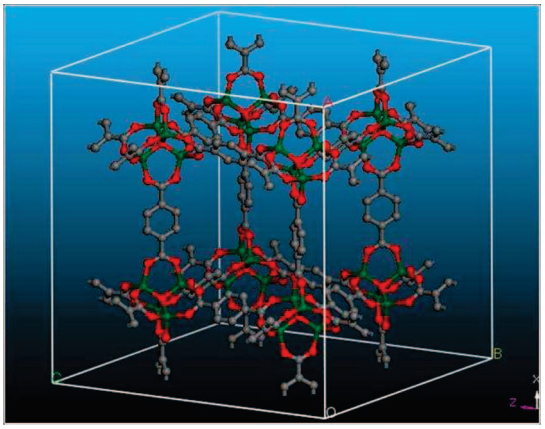

Figure 1. Unit cell structure of the Zn(BDC) (IRMOF-1) as represented with the Material Studio software platform.

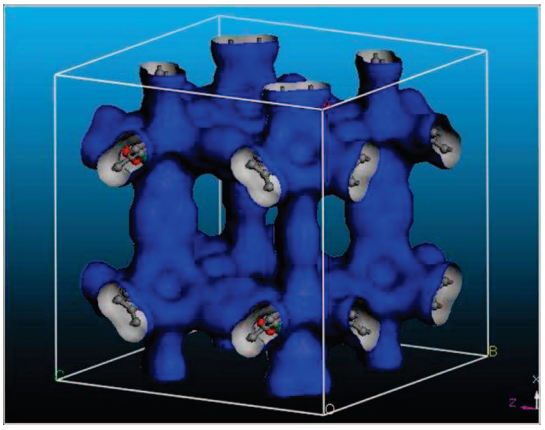

Figure 2. Surface area of the Zn(BDC) as illustrated using the Connolly method.

usually provide a good indication of the extent of adsorption sites as it is demonstrated for activated carbons and zeolites.[3,4] Good correlations between these quantities were also obtained on a set of MOFs.[5] Microporous MOFs provide strong confinement of the guest species, with pores of dimensions inferior to 2 nm. Whether the BET method determines actual geometric areas is questionable and, in such case, the surface area may be qualified as "apparent".[6] In fact, owing to confinement in micropores, the potential wells from opposite walls can overlap which results in micropore filling by a liquid.[7] This phenomenon has been observed in several MOFs in the 50−100 K range.[8−10] More specifically, the adsorbed hydrogen phase near pore saturation was found to behave like an incompressible fluid and to reach bulk liquid densities.[8−10] The isotherms revealing these typical liquid state properties could be modeled successfully using a Dubinin−Astakhov micropore filling equation. Hence, as assumed in earlier works, such mechanism is not restricted to subcritical temperatures.[11] These investigations have shown how the determination of some thermodynamic properties of the adsorbed phase near saturation can reveal both the physical limits of the adsorbent and its influence on the guest molecules. The aim of the present study is to get further experimental insights on the nature and on the behavior of the adsorbed hydrogen phase in MOFs in connection with their specific surface area, structure and chemical functionality. The influence of the structure and composition of the adsorbents on the nature of the adsorbed phase is investigated in that perspective. The approach involves the synthesis of an extended set of MOFs along with the measurement and analysis of their excess hydrogen adsorption isotherms, and their porosity. Traditional adsorbents such as activated carbons and molecular sieves were also tested for comparison. Hydrogen adsorption measurements were performed between 77 and 50 K inclusively. The saturation behavior could be observed at 50 K, allowing for a direct calculation of the adsorbed phase densities and volumes, and the corresponding absolute isotherms. These quantities were used to investigate the state of the adsorbed supercritical hydrogen. The results are discussed in the perspective of on-board hydrogen storage.

2. Theoretical Background

Solid−gas adsorption consists essentially of the enrichment of guest molecules (i.e., adsorbate), in the vicinity of the surface of a solid over the concentration of the bulk gas phase. The total amount of adsorbate molecules present in the space V_a in which the attractive field from the surface is effective is referred to as the absolute amount adsorbed N_a defined as[12]

$$N_a = \int_{Va} \rho_a \, dV \tag{1}$$

where ρ_a is the density of the adsorbed phase. The amount N_a generally eludes experiments because the spatial extension (V_a) of the adsorbed phase is not measurable under usual (P, T) conditions. In fact, adsorption measurements are commonly performed with reference to a nonadsorbing system and the corresponding measured quantity is referred to as the excess amount adsorbed N_{ex}.[13] The latter corresponds to the fraction of all the adsorbate molecules in V_a which is solely owed to solid−gas interactions. N_a and N_{ex} are formally related as

$$N_{ex} = \int_{Va} (\rho_a - \rho_g) \, dV \tag{2}$$

N_{ex} is characterized by a maximum that occurs when ρ_a approaches monotonically a constant value while the gas density ρ_g continues to increase proportionally to the pressure. Therefore, N_{ex} exhibits near saturation a characteristic decrease from which adsorbed phase properties can be studied. Given that sufficient data are available near saturation (e.g., at very low temperature and relatively high pressure), the volume V_a occupied by the adsorbed phase can be extracted as[8−10,14]

$$-\frac{dN_{ex}}{d\rho_g} \cong V_a \text{ for } N_a \rightarrow \text{constant} \tag{3}$$

If eq 3 behaves linearly, that is V_a does not change with pressure, one may then conclude that the adsorbed phase behaves

(3) Chahine, R.; Bose, T. K. *Hydrogen Energy Progress XI*; Veziroglu, T.N., et al., Eds.; International Association of Hydrogen Energy: Coral Gables, FL,1996; p 1259.
(4) Sing, K. *Colloids Surf., A* **2001**, *187−188*, 3–9.
(5) Hirsher, M.; Panella, B. *Scripta Mater.* **2006**, *56*, 809–812.
(6) Fletcher, A. J.; Thomas, K. M.; Rosseinsky, M. J. *J. Solid State Chem.* **2005**, *178*, 2491–2510.
(7) Dubinin, M. M.; Astakhov, V. A. *Izv. Akad. Nauk SSSR Ser. Khim.* **1971**, *1*, 5-11 (translated from Russian).
(8) Poirier, E.; Dailly, A. *J. Phys. Chem. C* **2008**, *112*, 13047–13052.
(9) Poirier, E.; Dailly, A. *Nanotechnology* **2009**, *20*, 204006.
(10) Poirier, E.; Dailly, A. *Energy Environ. Sci.* **2009**, *2*(4), 420–425.
(11) Amankwah, K. A. G.; Schwarz, J. A. *Carbon* **1995**, *33*, 1313–1319.
(12) Rouquerol, F.; Rouquerol, J.; Sing, K. *Adsorption by Powders and Porous Solids*; Academic Press: London, 1999.
(13) Bénard, P.; Chahine, R. *Langmuir* **2001**, *17*, 1950–1955.
(14) Menon, P. G. *Chem. Rev.* **1968**, *68*, 277–294.

like an incompressible fluid. In this case, the decrease of the excess isotherm near saturation can be directly associated with the displacement of gas by the adsorbed phase. The density of the adsorbed phase can be approximated from the expression

$$\rho_a \cong \frac{N_{ex}}{V_a} + \rho_g \quad (4)$$

Equation 4 reduces to $\rho_a \cong \rho_g$ when $N_{ex} = 0$, reflecting that no "gain" over compression is made when the gas density is high enough. In the absence of phase transition, neither V_a nor ρ_a should vary in the saturation regime. This will be verified later by performing linear analysis of the isotherms near saturation, and extrapolating down to $N_{ex} = 0$. The quantities V_a and ρ_a are closely related to the underlying physics of the system and its ability to adsorb hydrogen.[15] They can reveal of the effects of chemical functionality, pore size and gas-gas interactions. Moreover, V_a can be used to calculate N_a by means of eqs 3 and 4 as

$$N_a \cong N_{ex} + \rho_g V_a \quad (5)$$

This amount representing a measure of the adsorption capacity of the microporous material is thus calculated, in contrast with usual approaches, without independent assumptions about the porous volume of the adsorbent (e.g., crystallographic volume). The quantity ρ_a provides a basis for the calculation of the mean spacing between adsorbed molecules, and quantum effects. The classical or quantum nature of the adsorbed hydrogen can be identified using the de Broglie thermal wavelength, which is defined as[16]

$$\Lambda = \left(\frac{2\pi\beta\hbar^2}{m}\right)^{1/2} \quad (6)$$

where $\beta = (k_b T)^{-1}$ and $\hbar = h/2\pi$, m is the mass of a particle, k_b and $\hbar$ are respectively the Boltzmann and Planck constants. Λ is usually compared with the mean spacing between hydrogen molecules, a_0, which can be deduced from ρ_a as $a_0 \cong \rho_a^{-1/3}$. A classical treatment is valid if Λ is much smaller than a_0, that is $\Lambda/a_0 \ll 1$; otherwise quantum effects can be considered. Because the quantum behavior of molecules tends to increase their effective diameter, it can oppose the densification of the adsorbed phase and limit the performances of hydrogen storage adsorbents.

3. Experimental Section

3.1. Materials. In this study we examine the hydrogen adsorption properties of a large number of MOFs composed of different inorganic clusters and linking organic units. All laboratory scale samples were prepared via a one-pot reaction by solvothermal methods from a solution or slurry of the metal ion salt with the corresponding linking organic unit. MOFs for hydrogen storage purposes have extended three-dimensional structures with structural stability incorporating uniform pores and a network of channels. The activation of the porosity was achieved by the removal of noncoordinating guests' species like solvent molecules in the pores and channels. A substantial number of porous MOFs were evaluated for their excess hydrogen uptake. The first group of materials we studied is first-generation MOFs based on aromatic carboxylate ligands such as BDC (1,4-benzenedicarboxylate),[17−20] BTB (4,4′,4″-benzene-1,3,5-triyl-tribenzoate),[21,22] TTDC (thieno[3,2-b]thiophene −2,5- dicarboxylate),[23] TCN (3,5,3′,5′-tetracarboxylate naphthalene),[24] TCP (3,5,3′,5′-tetracarboxylate phenanthrene),[24] TPTC (terphenyl 3,5,3′,5′-tetracarboxylate),[25] QPTC (quaterphenyl 3,3‴,5,5‴-tetracarboxylate),[25] BTC (1,3,5-benzenetricarboxylate),[26,27] and DOBDC (2,5-dihydroxy-1,4-benzenedicarboxylate).[28] We also have examined microporous coordination solids analogous to the MOFs where carboxylate ligands are replaced by structurally analogous functional nitrogen-based bridging ligands while essentially keeping the same specific surface area. The linking organic units are BDP (1,4-benzenedipyrazolate), BTT (1,3,5-benzenetristetrazolate),[29] TPT-3tz (2,4,6-tri-p(tetrazol-5-yl)phenyl-s-triazine),[30] and TTPM (tetrakis (4-tetrazolylphenyl) methane).[31] Finally we explored two MOFs based on metal imidazolates: PhIM (benzimidazolate) and MeIM (2-methylimidazolate).[32] The molecular structures of the mentioned extended ligands are shown in Figure 3. Considering that some MOFs are known to be air/moisture sensitive, they were systematically handled under inert atmosphere (argon).[33] AX-21, a well-known coconut shell KOH-activated carbon obtained from AK Research Inc., as well as a type Y molecular sieve, obtained from Alfa Aesar, were also tested for comparison purposes.

3.2. Hydrogen Sorption and Specific Surface Area Measurements. The samples were degassed for about 24 h under high vacuum up to 373 K prior to each adsorption experiment. The hydrogen adsorption isotherms were measured using an automated Sieverts' apparatus (PCT-Pro 2000 from Hy-Energy LLC). The system involves a liquid helium flow cryostat we have adapted to control precisely the temperature in the pressurized cell within $\Delta T = 10$ mK over the whole 50−300 K range. The amount of gas adsorbed in excess was calculated from a set of gas expansion by comparing the amount of hydrogen sent to the sample cell with the amount of residual gaseous hydrogen in the same cell after each expansion. The differences between these two quantities were summed as a function of pressure to build the excess adsorption isotherms. The equilibrium conditions were carefully identified using graphical plotters that monitor the system pressure and the temperature as a function of time. The dead space volumes were determined at room temperature using helium as a negligibly adsorbing gas. Ultrahigh purity hydrogen and helium (99.999% purity) obtained from Airgas Inc. were used. The porosity of the

(15) Frost, H.; Snurr, R. Q. *J. Phys. Chem. C* **2007**, *111*, 18794–18803.
(16) Kowalczyk, P.; Holyst, R.; Terzyk, A. P.; Gauden, P. A. *Langmuir* **2006**, *22*, 1970–1972.
(17) Li, H.; Eddaoudi, M.; O'Keeffe, M.; Yaghi, O. M. *Nature* **2008**, *402*, 276–279.
(18) Barthelet, K.; Marrot, J.; Riou, D.; Ferey, G. *Angew. Chem. Int. Ed.* **2002**, *41*(2), 281–284.
(19) Ferey, G.; Mellot-Draznieks, C.; Serre, C.; Millange, F.; Dutour, J.; Surble, S.; Margiolaki, I. *Science* **2005**, *309*, 2040–2042.
(20) Loiseau, T.; Serre, C.; Huguenard, C.; Fink, G.; Taulelle, F.; Henry, M.; Bataille, T.; Ferey, G. *Chem.—Eur. J.* **2004**, *10*, 1373–1382.
(21) Furukawa, H.; Miller, M. A.; Yaghi, O. M. *J. Mater. Chem.* **2007**, *17*(30), 3197–3204.
(22) Chen, B. L.; Eddaoudi, M.; Hyde, S. T.; O'Keeffe, M.; Yaghi, O. M. *Science* **2001**, *291*(5506), 1021–1023.
(23) Rowsell, J. L. C.; Yaghi, O. M. *J. Am. Chem. Soc.* **2006**, *128*, 1304–1315.
(24) Yang, S. H.; Lin, X.; Dailly, A.; Blake, A. J.; Hubberstey, P.; Champness, N. R.; Schroder, M. *Chem.—Eur. J.* **2009**, *15*(19), 4829–4835.
(25) Lin, X.; Telepeni, I.; Blake, A. J.; Dailly, A.; Brown, C. M.; Simmons, J. M.; Zoppi, M.; Walker, G. S.; Thomas, K. M.; Mays, T. J.; Hubberstey, P.; Champness, N. R.; Schroder, M. *J. Am. Chem. Soc.* **2009**, *131*(6), 2159–2171.
(26) Mueller, U.; Schubert, M.; Teich, F.; Puetter, H.; Schierle-Arndt, K.; Pastre, J. *J. Mater. Chem.* **2006**, *16*, 626–636.
(27) Loiseau, T.; Lecroq, L.; Volkringer, C.; Marrot, J.; Ferey, G.; haouas, M.; Taulelle, F.; Bourrelly, S.; llewelly, P. L.; Latroche, M. *J. Am. Chem. Soc.* **2006**, *128* (31), 10223–10230.
(28) Caskey, S. R.; Wong-Foy, A. G.; Matzger, A. J. *J. Am. Chem. Soc.* **2008**, *190*, 10670–10671.
(29) Dinca, M.; Dailly, A.; Liu, Y.; Brown, C. M.; Neumann, D. A.; Long, J. R. *J. Am. Chem. Soc.* **2006**, *128*(51), 16876–16883.
(30) Dinca, M.; Dailly, A.; Tsay, C.; Long, J. R. *Inorg. Chem.* **2008**, *14*(1), 11–13.
(31) Dinca, M.; Dailly, A.; Long, J. R. *Chem.—Eur. J.* **2008**, *14*(33), 10280–10285.
(32) Park, K. S.; Ni, Z.; Cote, A. P.; Choi, J. Y.; Huang, R.; Uribe-Romo, F. J.; Chae, H. K.; O'Keeffe, M.; Yaghi, O. M. *Proc. Natl. Acad. Sci.* **2006**, *103*(27), 10186–10191.
(33) Kaye, S. S.; Dailly, A.; Yaghi, O. M.; Long, J. R. *J. Am. Chem. Soc.* **2007**, *129*, 14176–14177.

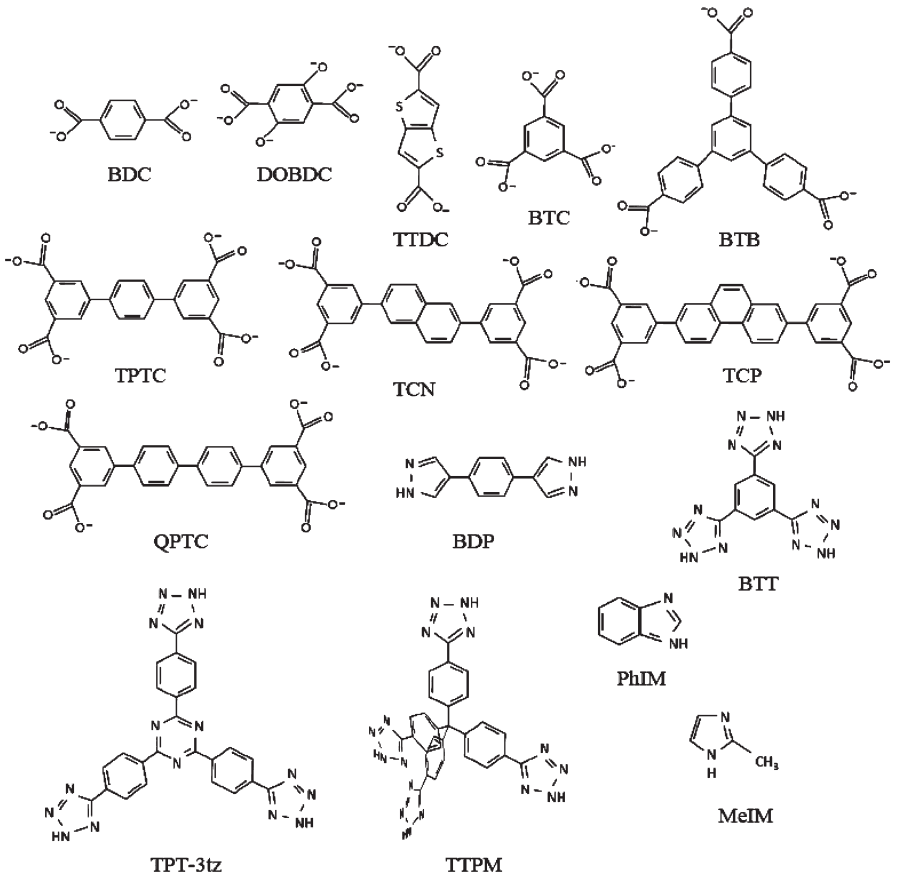

Figure 3. Organic linkers used in the coordination frameworks presented in this study.

activated materials was measured using a Quantachrome Autosorb-1 automated gas-sorption apparatus. The specific surface areas of the samples were evaluated from nitrogen sorption isotherms at 77 K using the BET model. The total pore volumes were extracted from argon adsorption isotherms measured at 87 K.

4. Results and Discussion

4.1. Excess Hydrogen Adsorption at 77 K. A significant set of data, including excess isotherms of hydrogen adsorption and desorption, maximum hydrogen uptakes as well as Brunauer−Emmett−Teller (BET) specific surface areas (N_2), have been measured. The 77 K excess hydrogen adsorption isotherms were performed at pressures up to 60 bar for an extended range of MOFs materials. Note the hydrogen excess adsorption uptakes are reported in specific units, mass of hydrogen per gram of adsorbent (mg g^{-1}), to allow a consistent comparison on the same basis than the surface area units. As expected from a physisorption process, the hydrogen adsorption isotherms were completely reversible for all the samples except for Al(BDC) and Co(BDP); which showed hysteretic behaviors, as discussed later. In most cases, the process was fast and hydrogen was adsorbed in less than 5 min. The samples could also be regenerated by degassing at room temperature, showing weak solid−gas interactions. The materials showed reproducible hydrogen uptakes following several of such adsorption/desorption cycles, revealing their structures were stable in that respect. Figure 4 presents a survey of the maximum excess hydrogen storage uptakes measured at 77 K as a function of the BET specific surface areas. The metal ion of the SBU and the linking organic unit are indicated for each studied MOF. The higher maximum excess hydrogen uptakes measured

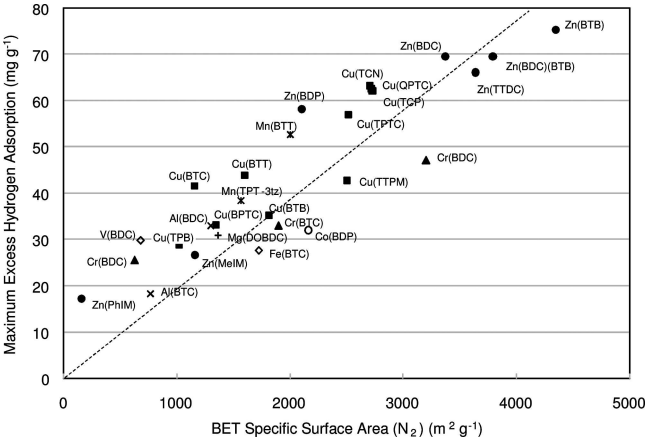

Figure 4. Maximum excess hydrogen uptakes measured at 77 K versus BET specific surface areas for different types of MOFs.

at 77 K range between 6 and 7.5 wt % for Zn(BTB) (MOF-177), Zn(BDC)(BTB) (UMCM-1), Zn(BDC) (IRMOF-1), and Zn(TTDC) (IRMOF-20). These MOFs, with very high surface areas, i.e., exceeding 3000 m^2 g^{-1}, can visibly store more hydrogen by weight than any of the other microporous materials presented. They also surpass the well-known AX-21 activated carbon, which is limited to about 5.5 wt % hydrogen in excess at 77 K. This illustrates that MOFs, as an emerging technology, have significant capabilities for molecular hydrogen storage on a gravimetric basis.

The maximum excess hydrogen uptakes correlate with the BET surface areas as evidenced by the trend curve shown in Figure 4.

Table 1. Summary of Hydrogen Adsorption Measurements at 50 K and Structural Properties[a]

sample	N_{ex}^{max} (mg·g^{-1})	A_{BET} (m^2 g^{-1})	V_a (mL g^{-1})	V_p^{Ar} (mL g^{-1})	ρ_a^{max} (g·L^{-1})	N_a^{max} (mg·g^{-1})
Zn(BDC)	90	3370	1.56	1.48	67	100
Zn(BTB)	105	4343	2.2	1.88−2.00	56	130
Cu(BPTC)	39	1346	0.91	0.78	51	46
Cu(TPTC)	69	2514	1.4	0.96	55	79
AX-21	74	2900	1.52	1.33	61	93
MS	19	900	0.42	0.25	54	23

[a] Note that N_{ex}^{max}: maximum excess hydrogen uptake; A_{BET}: BET specific surface area; V_a: adsorbed hydrogen phase volume; V_p^{Ar}: porous volume measured with Argon; ρ_a^{max}: maximum adsorbed hydrogen phase density; N_a^{max}: maximum absolute hydrogen uptake.

The curve has a slope of $m_0 = 0.02 \pm 0.002$ mg m^{-2} or 1 ± 0.1 wt % per 500 m^2 g^{-1}. This value corresponds essentially to Chahine's rule established for activated carbons and zeolites.[3] This correlation is therefore quite independent of the type of material. Present data were indeed obtained on qualitatively different materials, including porous frameworks built from the linking of different building blocks and organic units with different functionalities. The error on the presented trend is, in part, inherent to the BET method.[34] It can also be associated to the presence of a relatively high number of very small pores in some materials. Because of their larger molecular size, the nitrogen molecules used for the BET measurement might not access the same adsorption sites that are available to hydrogen.[35,36] The Zn(PhIM) may be an example of this phenomenon. Moreover, some variability in the trend may also occur because of micropore filling and differences in adsorbate packing densities. As revealed in a previous report, the adsorbed phase density of hydrogen may vary up to 40% on different materials near saturation at 50 K.[9] This aspect will now be further investigated.

4.2. Excess Hydrogen Adsorption Measurements at 50 K. In order to get further insights into the nature of the adsorbed phase and its influence on the correlation with the surface area, the excess adsorption isotherms of some specific microporous materials were analyzed close to saturation at 50 K. It can be assumed that the adsorption mechanism and the state of the adsorbed hydrogen at 50 K are basically the same as those at 77 K, as already observed on Zn(BDC), Zn(BTB), Cu(TPTC), and Cu(BPTC).[8−10] The hydrogen adsorption isotherms on each of these materials were, in fact, successfully modeled with a same set of Dubinin-Astakhov model parameters over the 50−77 K range. The applicability of the model is owed to the small pore sizes in these materials, which are about 1.7, 1.5, 0.73, and 0.65 nm respectively for the Zn(BDC), Zn(BTB), Cu(TPTC), and Cu(BPTC).[21,37,38] In this section, these materials are studied side by side and compared with the AX-21 activated carbon and a type Y molecular sieve (MS). Chemically, the Cu-MOFs have open metal sites which make them interesting because of their enhanced affinity for guest species.[39] Consistent with eqs 3 and 4, the measured excess adsorption isotherms are expressed in Figure 5 as a function of the gas phase density.[40] The behaviors of the isotherms at low filling (pressures) vary for the different samples, likely as a result of variations in hydrogen affinity due to chemical differences in the organic units.[41] For instance, the higher affinity for molecular hydrogen in the open metal sites materials such as the Cu-based MOFs is a likely cause of a steeper increase of adsorption as a function of pressure.[41] In the near saturation region, observed past the excess maxima, the excess isotherms on all the materials eventually exhibit a linear regime ($R^2 > 0.995$) as a function of ρ_g. In accordance with eq 3, this remarkable feature indicates that an incompressible adsorbed phase is formed on all of the present samples. From that standpoint, it is interesting to note that the adsorbed hydrogen phase on the MOFs does not differ from that on the traditional adsorbents (i.e., AX-21 and MS). The adsorbed phase volumes and densities were calculated using eqs 3 and 4 in the saturation regions of the 50 K excess isotherms; the results are presented in Table 1. These adsorbed phase volumes are, in many cases, consistent with the volumes measured using argon porosimetry, which are also presented in the table for comparison. It was observed that the values of adsorbed hydrogen phase volumes exceed to some extent that of reported porous volumes calculated from crystallographic data. However, the volume ratios between samples are comparable using either quantity, e.g., in the case of the Cu-MOFs one finds $V_a^{(BPTC)}/V_a^{(TPTC)} = 0.63$; the same ratio can be obtained using the porous volumes calculated by Lin et al. from crystallographic data (i.e., using $V_p^{(BPTC)} = 0.68$ and $V_p^{(TPTC)} = 1.08$ mL g^{-1}).[38] The difference between these volumes and those measured using eq 3 might be due to defects and structural transformations such as stretching, rotational, "breathing" and scissoring mechanisms, which all can affect the structure.[42] These effects could possibly be exacerbated at the lowest temperatures. The adsorbed phase

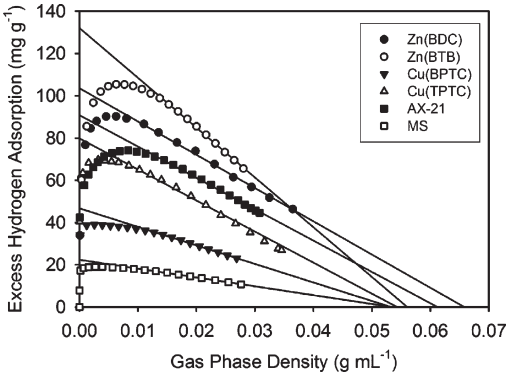

Figure 5. Plots of the measured excess hydrogen adsorption at 50 K expressed as a function of the gas density. The saturation regimes past the excess maxima were linearly fitted and extrapolated to $N_{ex} = 0$.

(34) Gregg S. J.; Sing K. S. W. *Adsorption, surface area and porosity*, 2nd ed.; Academic Press: New York, 1982.
(35) Poirier, E.; Chahine, R.; Bose, T. K. *Int. J. Hydrogen Energy* **2001**, *26*, 831–835.
(36) Ahn, C. C.; Ye, Y.; Ratnakumar, B. V.; Witham, C.; Bowman, R. C., Jr.; Fultz, B. *Appl. Phys. Lett.* **1998**, *73*, 3378–3380.
(37) Rowsell, J. L. C.; Yaghi, O. M. *Angew. Chem., Int. Ed.* **2005**, *44*, 4670–4679.
(38) Lin, X.; Jia, J.; Zhao, X.; Thomas, K. M.; Blake, A. J.; Walker, G. S.; Champness, N. R.; Hubberstey, P.; Schröder, M. *Angew. Chem., Int. Ed.* **2006**, *45*, 7358–7364.
(39) Panella, B.; Hirscher, M.; Putter, H.; Muller, U. *Adv. Funct. Mater.* **2006**, *16*, 520–524.
(40) Lemmon E. W.; Peskin A. P.; McLinden M. O.; Friend D. G. *NIST12 Thermodynamic and Transport Properties of Pure Fluids - NIST Standard Reference Database 23*, Version 8.0; U.S. Secretary of Commerce: Washington, DC, 2007.
(41) Rowsell, J. L. C.; Millward, A. R.; Park, K. S.; Yaghi, O. M. *J. Am. Chem. Soc.* **2004**, *126*, 5666–5667.
(42) Fletcher, A. J.; Thomas, K. M.; Rosseinsky, M. J. *J. Solid State Chem.* **2005**, *178*, 2491–2510.

densities invariably fall in the 50−70 g L^{-1} range for all materials. Notably, this range of densities corresponds to that of liquid hydrogen between 33 and 20 K for different saturation pressures.[40] In this view, differences in the affinities of the adsorbents for hydrogen seem to mimic changes in the equilibrium (P, T) conditions of the bulk liquid. An inspection of figure 5 also clearly shows that linear extrapolations down to $N_{ex} = 0$, where $\rho_a = \rho_g$, yield adsorbed phase densities consistent with those obtained using eq 4. It could be noted that both V_a and ρ_a become constant a little past the excess maxima, meaning the latter indicates well the beginning of the saturation regime. This feature is a remarkable effect of adsorption in micropores considering the bulk supercritical gas does not have a well-defined saturation pressure.

Interestingly, it is apparent from Figure 5 that the amount adsorbed rises steeply with increasing pressure on both Cu-(BPTC) and the MS. On the other hand, these samples also have the smallest adsorbed phase densities. These results suggest that a reduction of the pore size may not lead to any gain in the maximum hydrogen packing densities despite enhancing solid−gas interactions. For instance, this can be evidenced by considering the adsorbed phase density of Cu(BPTC) (51 g L^{-1}), which is smaller than that of Zn(BTB) (55 g L^{-1}), despite smaller pores. The behavior of the curves in Figure 5 is qualitatively comparable to the excess hydrogen adsorption isotherms for different slit pore widths calculated by Bénard et al. using a Grand Canonical Simulations approach.[43] In the present view, one advantage of the higher hydrogen affinity in small pores would be potentially milder (P, T) operating conditions. This aspect will be discussed in section 4.4 in relation to adsorption enthalpy calculations.

At the microscopic level, some limiting factors for the packing of molecules in small pores are associated with electronic repulsion between adsorbate molecules, and quantum effects. The latter become particularly important at low temperatures. The magnitude of such effect can be assessed using the de Broglie wavelength. For hydrogen at 50 K, eq 6 yields $\Lambda = 0.17$ nm. Considering the mean spacing between hydrogen molecules is $a_0 \cong \rho_a^{-1/3}$, then for the observed densities varying between 50 and 70 g L^{-1} one obtains $a_0 = 0.41-0.36$. Hence the ratio Λ/a_0 lies between about 0.4−0.5 showing the adsorbed hydrogen has a significant wave-like character. This phenomenon is likely to oppose the densification of the adsorbed phase and limit the hydrogen uptake in the present conditions.[9,44]

4.3. Absolute Adsorption Isotherms at 50 K. The previously calculated V_a and ρ_a values can be used to evaluate the absolute amounts adsorbed such as $N_a = \rho_a V_a$. The latter are presented for the specific set of samples in the last column of Table 1. On this basis, considerable amounts can be stored at 50 K, up to 25% more than the maximum excess values. In particular, a substantial capacity of about 12 wt % is reached on the Zn(BTB). The extent of the absolute uptake is mainly determined by the adsorbed phase volume. Note that ρ_a appears as a relatively less important factor to reach high hydrogen storage capacities as it does not vary as much as V_a with respect to the materials' type. The particular absolute isotherms, obtained using eq 5, along with their excess counterparts are plotted, for example, for the Zn(BTB) and Cu(BPTC) in Figure 6. Both absolute isotherms are of type I and clearly exhibit the typical

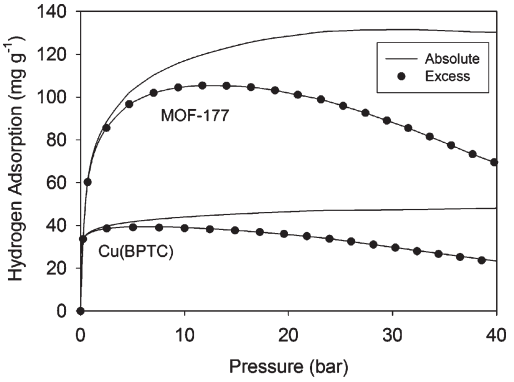

Figure 6. Plots of excess and absolute isotherms on Zn(BTB) and Cu(BPTC) at 50 K.

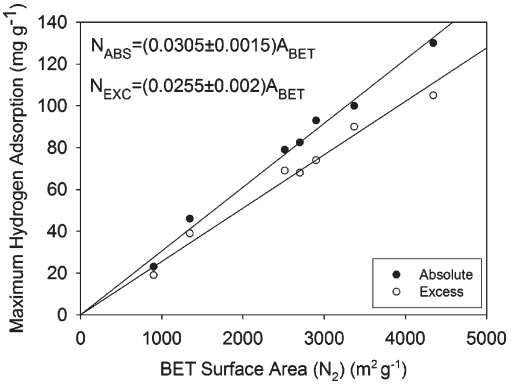

Figure 7. Absolute and excess amounts adsorbed at 50 K as a function of the BET specific surface area.

monotonic behavior associated with a saturation regime at high pressure. The comparatively lower performance of Cu(BPTC) is, as exposed in the previous section, a consequence of reduced V_a and ρ_a values on this material.

Figure 7 expresses the maximum absolute and excess amounts adsorbed at 50 K as a function of the BET surface area for a set of adsorbents including those presented in Table 1. A linear correlation can also be established between these quantities. The correlation obtained with the absolute amount is slightly better than the one using the excess one as evidenced from the regression error on the slopes. Also, in the case of excess adsorption, the slope, $m_0 = 0.0255$ mg m^{-2}, is about 25% higher than that obtained at 77 K (i.e., 0.02 mg m^{-2}). This is naturally a result of the higher excess adsorption maxima at 50 K which, in turn, might be due to an increasing contribution of weakly attractive sites as the temperature decreases.

The variability in these curves can possibly be explained by differences in the hydrogen packing densities and by the occurrence of micropore filling. The later may be quantitatively equivalent to the superposition of adsorbed layers in the pores. In order to investigate this matter one may consider the mean lateral spacing between adsorbed molecules deduced from the apparent "surface" coverage. In essence, this quantity can be estimated as $\tilde{a}_0 \cong (1/m_0)^{1/2}$. It is found from the slope of the absolute amount as a function of the BET surface area that $\tilde{a}_0 = 0.32$ nm. This spacing is smaller than the previous spacing calculated from the adsorbed phase densities and, in fact, it is even smaller than under a solid hydrogen density. This unlikely result suggests the microporous space above the surface might be filled, leading to an overestimation of apparent surface coverage. It is interesting to consider the following approximation regarding

(43) Bénard, P.; Chahine, R.; Chandonia, P. A.; Cossement, D.; Dorval-Douville, G.; Lafi, L.; Lachance, P.; Paggiaro, R.; Poirier, E. *J. Alloys Compd.* **2007**, *446−447*, 380–384.
(44) Garberoglio, G.; Skoulidas, A. I.; Johnson, J. K. *J. Phys. Chem. B* **2005**, *109*, 13094–13103.

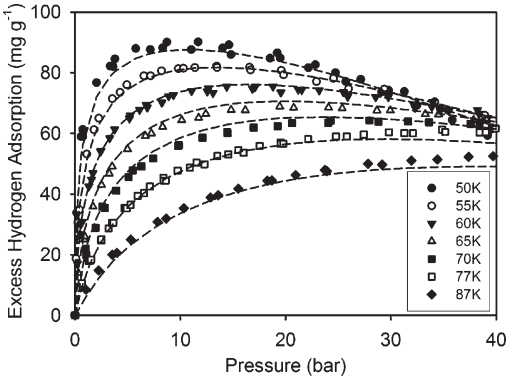

Figure 8. Measured (data points) and modeled (dashed) excess adsorption isotherms on Zn(BDC) over the 50−87 K range (adapted from ref 8). A form of the Dubinin−Astakhov equation adapted for excess adsorption was used for modeling.

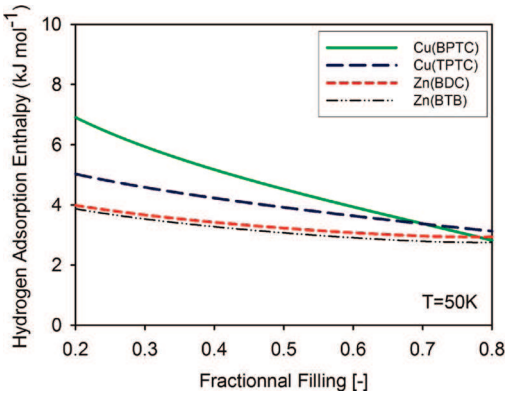

Figure 9. Magnitude of the hydrogen adsorption enthalpy at 50 K as a function of filling on Zn- and Cu-based MOFs.

the surface area (A_{BET}) and the pore volume: $V_a(A_{BET})^{-1} \cong na_0$, where the quantity n would represent the "apparent" number of layers of adsorbed molecules above the surface in the pores. Using the tabulated V_a and A_{BET} values, and the previously calculated a_0 = 0.36−0.41, one find that $n \cong 1.2-1.7$. The different n values can be interpreted as various "stacking" arrangements of adsorbed molecules in the pores. These different arrangements may also be related to the variability in trends relating the amounts adsorbed and the BET surface areas.

4.4. Adsorption at Different Temperatures. In order to assess the magnitude of the solid−gas interactions and their influence on hydrogen uptakes, adsorption at different temperatures has been examined. Excess hydrogen adsorption on Zn(BDC), Zn(BTB), Cu(BPTC), and Cu(TPTC) materials has been previously measured between 50 and 87 K and up to 40 bar.[8−10] The isotherms measured on this set of MOFs materials were also successfully modeled using the Dubinin−Astakhov micropore filling equation in a form adapted for excess adsorption. Figure 8 is an example of hydrogen adsorption isotherms obtained over the above-mentioned (P, T) range.[8] The parametrization of the (P, T) dependence of the amount adsorbed allowed for the calculation of the adsorption enthalpy as a function of fractional filling and temperature using the Clausius−Clapeyron equation. Note the complete modeling approach was described in details in previous articles.[8−10] The magnitude of the adsorption enthalpy (ΔH) at 50 K is presented in Figure 9 for the different MOFS. The material with the smaller pore size, Cu(BPTC), shows the highest ΔH, in accordance with the steep increase of its isotherms as a function of pressure noted in section 4.2. All the enthalpies lie in a range of

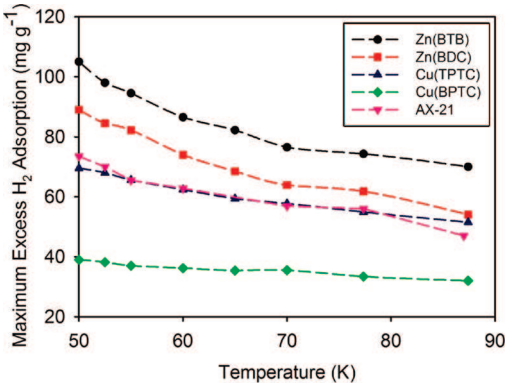

Figure 10. Profile of the excess adsorption maxima of various MOFs as function of temperature. The activated carbon AX-21 is also shown for comparison.

values consistent with physical types of interactions. The diminution of ΔH with fractional filling, particularly rapid for the material with smaller pores Cu(BPTC), may be due to more variability in the energetic heterogeneity. This observation suggests that adsorption in these conditions departs from a mechanism in which the interaction energy is constant as a function of the coverage (e.g., Langmuir model). The influence of the enthalpy on the amounts adsorbed is revealed by comparing how the excess maxima vary as a function of temperature for the different materials, as shown in Figure 10.

This figure shows that amounts adsorbed by the Zn-based MOFs surpass considerably that of other adsorbents over the whole 50−87 K range. The Zn(BTB), for instance, has maximum hydrogen excess uptakes 30−40% larger than AX-21 activated carbon. The decrease of the curves with increasing temperature is likely a consequence of desorption from less attractive sites and of some dilution of the adsorbed phase. The MOF material with the shortest linker and the highest ΔH, i.e. Cu(BPTC), exhibits steadier maximum excess amounts with increasing temperature. Therefore, although reducing the pore size may not enhance the maximum adsorbed phase density, it favors the retention of the hydrogen as the temperature increases as a result of the stronger solid−gas interaction. This observation clearly exposes an inherent contradiction between the large pore volumes required to enhance hydrogen storage capacity and the resulting decrease in the strength of the interaction in larger pores. This conflict can be seen from the reverse order of the curves between Figures 9 and 10. Hence, the potential (P, T) operating conditions may be improved using a material with smaller pores, because of a higher ΔH, but at the cost of a reduction of pore volume while no gain is made in term of maximum adsorbed phase density. These conclusions are consistent with some recent independent theoretical calculations.[2] More experiments will be needed to determine if similar observations can be made beyond this particular set of materials.

5. Conclusions

Hydrogen adsorption measurements performed over an extended set of MOFs revealed fairly good correlations between the maximum excess amounts adsorbed at 77 and 50 K and the BET surface area. Such correlations suggest the nature of the adsorbed phase near saturation is essentially independent of the structure and the chemical composition of the adsorbents. This observation is supported by measurements at 50 K which showed that the adsorbed phase behaves like an incompressible fluid reaching bulk liquid state densities (50−70 g L^{-1}). This behavior, found on

a set of qualitatively different samples, shows the adsorbed phase near saturation is not altered much by differences in the sample's affinity for molecular hydrogen. The variability (~10%) in the correlation between the maximum hydrogen uptake and the surface area can be explained by variations in the adsorbate packing consistent with the above-cited range of bulk liquid hydrogen densities. The present conclusions on the state of the adsorbed hydrogen are consistent, in essence, with simulation results.[45,46] The usual assumption of monolayer coverage of hydrogen near saturation does not seem to hold in the present conditions. The stronger hydrogen affinity on the materials with smaller pores leads to a displacement of the excess maximum to lower pressures and to a steadier adsorption capacity as a function of temperature. However, the enhancement of the solid−gas interactions does not necessarily lead to higher packing of molecular hydrogen, as it is sometimes supposed. Hence, (P, T) adsorption conditions can be somehow milder on the materials with small pore widths, but at the cost of severe reductions in pore volumes and storage capacities. The determination of the adsorbed phase volumes allowed for the calculation of the absolute isotherms which were found to reach values up to 25% higher than their excess counterparts. This leads to substantial storage capacities, reaching 10−12 wt % at 50 K, on materials with large pore volumes already capable of adsorbing large excess amounts. The absolute amounts were also found to correlate well with the surface areas, showing the adsorbed phase properties are compatible with surface area considerations. Owing to the rapid evolution of this class of material, it seems likely that new MOFs could have higher storage capacities, mitigating the efficiency penalties associated with low operating temperatures. In particular, MOFs with a lower framework mass could be particularly interesting for on-board applications. From the present standpoint, such feature could compensate for potential limits to the densification of the adsorbed phase. On the other hand, strategies to retain hydrogen at higher temperatures are also being explored actively.[47,48] Flexible MOFs also have shown some interesting features for hydrogen storage. For instance, the adsorption/desorption curve of Al(BDC), also known as MIL-53 Al, presents an hysteresis that was recently explained by a structural transition between an open-pore to a close-pore structure as a function of temperature.[49] The material Co(BDP) also shows a significant hydrogen uptake with wide hysteresis consistent with an accordion-type flexible behavior of the channel pores.[50] Such unusual behaviors offer interesting paths to tailor adsorbent for specific (P, T) operating conditions.

Acknowledgment. The authors are grateful to Dr. Xiang Lin and Prof. Martin Schröder of the University of Nottingham (U.K.) and to Dr. Mircea Dinca and Prof. Jeffrey Long of University California Berkeley for providing some of the samples.

(45) Belof, J. L.; Stern, A. C.; Eddaoudi, M.; Space, B. *J. Am. Chem. Soc.* **2007**, *129*, 15202–15210.
(46) Belof, J. L.; Stern, A. C.; Space, B. *J. Phys. Chem. C* **2009**, *113*(21), 9316–9320.
(47) Li, Y.; Yang, R. T. *J. Am. Chem. Soc.* **2006**, *128*, 8136–8137.
(48) Han, S. S.; Goddard, W. A., III. *J. Am. Chem. Soc.* **2007**, *129*, 8422–8423.
(49) Liu, Y.; Her, J.-H.; Dailly, A.; Ramirez-Cuesta, A. J.; Neumann, D. A.; Brown, C. M. *J. Am. Chem. Soc.* **2008**, *130*, 11813–11818.
(50) Choi, H. J.; Dinca, M.; Long, J. R. *J. Am. Chem. Soc.* **2008**, *130*, 7848–7850.